

Parameterization of light absorption by components of seawater in optically complex coastal waters of the Crimea Peninsula (Black Sea)

Egor V. Dmitriev,^{1,*} Georges Khomenko,¹ Malik Chami,² Anton A. Sokolov,¹
Tatyana Y. Churilova,³ and Gennady K. Korotaev⁴

¹Laboratoire de Physico-Chimie de l'Atmosphère, UMR CNRS 8101, Maison de la Recherche en Environnement Industriel de Dunkerque, Université du Littoral Côte d'Opale, 189A Avenue Maurice Schumann, 59140 Dunkerque, France

²Laboratoire d'Océanographie de Villefranche, 06234 Villefranche sur Mer Cedex, France

³Institute of Biology of the Southern Seas, National Academy of Sciences of Ukraine, 2 Nakhimov Avenue, Sevastopol 99011, Crimea, Ukraine

⁴Marine Hydrophysical Institute, National Academy of Sciences of Ukraine, 2 Kapitanskaya Street, Sevastopol 99011, Crimea, Ukraine

*Corresponding author: yegor@mail.ru

Received 13 August 2008; revised 14 January 2009; accepted 14 January 2009;
posted 16 January 2009 (Doc. ID 100116); published 23 February 2009

The absorption of sunlight by oceanic constituents significantly contributes to the spectral distribution of the water-leaving radiance. Here it is shown that current parameterizations of absorption coefficients do not apply to the optically complex waters of the Crimea Peninsula. Based on *in situ* measurements, parameterizations of phytoplankton, nonalgal, and total particulate absorption coefficients are proposed. Their performance is evaluated using a log-log regression combined with a low-pass filter and the non-linear least-square method. Statistical significance of the estimated parameters is verified using the bootstrap method. The parameterizations are relevant for chlorophyll *a* concentrations ranging from 0.45 up to 2 mg/m³. © 2009 Optical Society of America

OCIS codes: 010.1030, 010.4450.

1. Introduction

The absorption of sunlight by particulate and dissolved matters in the ocean significantly contributes to the spectral distribution of the water-leaving radiance. The inverse dependence of the remote sensing reflectance on the total spectral absorption coefficient together with the distinctive characteristics of the oceanic constituents provides the physical basis for ocean color algorithms for determining their concentration from satellite measurements. The inversion of the remote sensing reflectance to retrieve concentrations of materials of interest (i.e., sus-

pended sediments, chlorophyll, organic matter, and suspended organic detritus) requires the development of bio-optical models consisting of establishing relationships between the constituent concentrations and the optical properties of the particles. The absorption coefficient of the hydrosols is partitioned into absorptions due to phytoplankton pigments, colored dissolved organic matter (CDOM), and nonalgal particles (NAPs).

During the past two decades, several field experiments devoted to the study of the spectral signature of phytoplankton absorption coefficients in various aquatic environments have been carried out [1–4]. In open ocean waters, hereafter referred to as Case I waters [5], the spectral variation of the phytoplankton absorption coefficient as a function of the

chlorophyll a concentration is thoroughly studied in [6,7]. In coastal waters, hereafter referred to as Case II waters [5], the bio-optical models were poorly documented over a long period of time. An extensive analysis of light absorption coefficients for a large data set collected in various European coastal waters is provided in [8]. In particular, Babin *et al.* [8] proposed parameterizations of the NAP and CDOM absorption properties for coastal zones. However, the parameterization of phytoplankton absorption coefficient with respect to chlorophyll concentration has still not been extensively studied in optically complex waters. The goal of the current paper is to study the variability in the spectral absorption coefficients of the particulate and dissolved components in coastal waters whose optical properties significantly depart from those measured by Babin *et al.* [8]. We especially focus on the relationship between the absorption properties of the phytoplankton and the pigment concentration. The analysis is conducted based on field measurements collected in the Black Sea coastal zone off the Crimea Peninsula, for which the variations of the optical properties of particles are presented and discussed in detail in [9–12].

First, a short description of the field experiment and the methods used for measuring the optical properties of the particles is presented. Second, bio-optical models for deriving the absorption coefficients of phytoplankton, NAPs, and CDOM are investigated. It is shown that the current parameterizations of spectral absorption coefficients [7,8] do not fit our data set. Therefore we propose new parameterizations of the absorption coefficients of phytoplankton, NAPs, and CDOM, which could be applicable for coastal waters showing similar optical features as those observed in Black Sea coastal zones. The parameterizations are obtained by applying different statistical methods. The performance of these methods is discussed and a rigorous analysis of the errors is performed. The stability and reliability of the retrieved parameters are verified.

2. Material and Methods of Measurements

In situ measurements of the optical properties of the particles were carried out during a field experiment that occurred in the Black Sea coastal area in the summer of 2002 [13]. Here we give a brief description of the experiment, and we refer to [9,10,14] for more details about the measurement techniques, calibration of devices, and weather conditions. The measurements were performed on an oceanographic platform located 600 m offshore from the southern Crimea coastline. The sample acquisition and processing were performed following the ocean optics protocols recommended for satellite ocean color sensor validation [15]. A total number of 132 seawater samples were collected at fixed depths, namely, 0, 4, 8, 12, 16, and 20 m. Concentrations of chlorophyll a (Chla) and phaeopigment (Phaeo) were determined using the standard fluorometric method [16]. The fluorometer was calibrated using known concentrations of

pure chlorophyll a. The samples (300–500 ml) were filtered through 25 mm glass fiber filters (Whatman GF/F). Pigments were extracted in 90% acetone in the dark at 6–8 °C for 18 h. The total chlorophyll a concentration (Tchla) is defined as the sum of Chla and Phaeo. It is known that the fluorometric measurements of these parameters may be perturbed by the presence of chlorophyll b in the samples [17]. On the basis of the data obtained near the platform in summer from 1996 to 2003, we have performed a taxonomic analysis of phytoplankton [18,19]. It was found that nano- and microphytoplankton is represented by different species of Bacillariophyceae, Dinophyceae, and Prymnesiophyceae classes. At the same time, the quantity of Chlorophyceae algae containing chlorophyll b and prochlorophytes containing divinyl chlorophyll b can be assumed to be negligible in the considered Black Sea coastal area.

The particulate absorption was measured using the methods described in [1,20]. The separation of the particulate absorption into phytoplankton and other components is based on the methanol extraction method [21]. The measurement made before the methanol extraction provides the total particulate absorption coefficient $a_p(\lambda)$, while the depigmented particle absorption coefficient $a_{\text{NAP}}(\lambda)$ is obtained after the extraction. The parameter $a_{\text{NAP}}(\lambda)$ is consistent with the absorption by the detrital particulate matter and is thus referred to as the NAP absorption coefficient. The phytoplankton absorption coefficient $a_{\text{ph}}(\lambda)$, which represents the absorption by the living particles, is obtained by the difference between $a_p(\lambda)$ and $a_{\text{NAP}}(\lambda)$. The spectral absorption of CDOM was measured with the dual beam spectrophotometer (SPECORD-M40, Carl Zeiss) using a 0.1 m long cuvette and deionized water as the reference. The water samples were filtered throughout 0.2 μm -pore-size membrane filters, which were first prerinsed with 50 ml of deionized water. The absorption was corrected for the instrument baseline, and the CDOM absorption coefficient $a_{\text{CDOM}}(\lambda)$ was calculated according to

$$a_{\text{CDOM}}(\lambda) = (\text{OD}_s(\lambda) - \text{OD}_{bs}(\lambda)) \cdot \ln 10, \quad (1)$$

where $\text{OD}_s(\lambda)$ is the optical density of the filtrate sample, and $\text{OD}_{bs}(\lambda)$ is the optical density of a purified water blank. Note that $\text{OD}(\lambda) = D(\lambda)/l$, where $D(\lambda)$ is the spectral absorbance, and l is the cuvette length (0.1 m here).

3. Results and Discussion

A. Local Absorption Budget

In the open ocean, the phytoplankton makes the major contribution to the absorption at 443 nm. In coastal waters, the absorption balance is much more variable. The relative contribution of phytoplankton, NAPs, and CDOM to the total absorption coefficient for the Black Sea coastal water was studied as a function of wavelength for 4 days, covering the entire

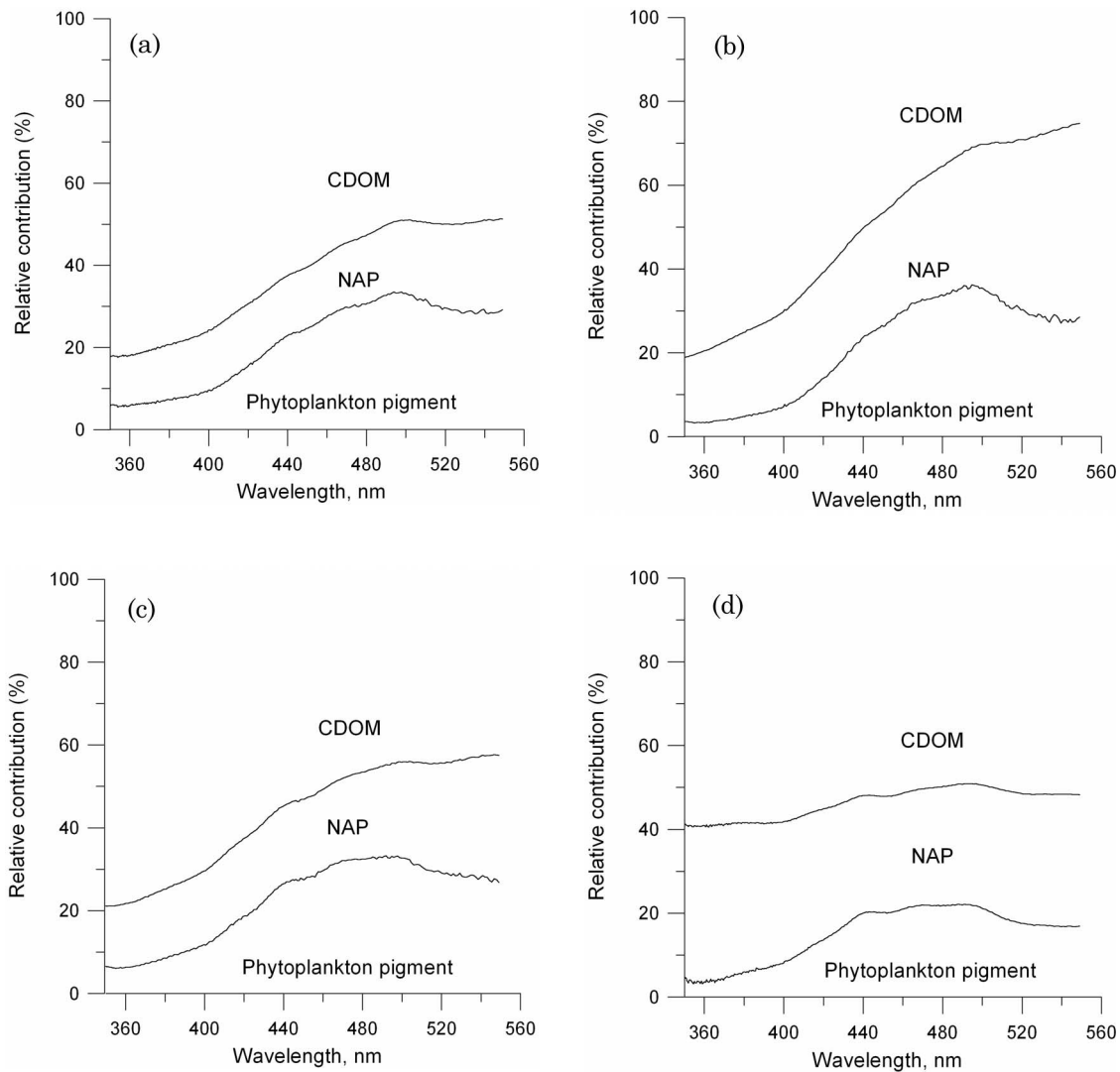


Fig. 1. Relative contribution of phytoplankton, NAPs, and CDOM absorption to the total absorption for (a) 2 August, (b) 3 August, (c) 10 August, and (d) 14 August 2002. The area between the x axis and the first lower curve represents the contribution of phytoplankton to the total absorption. The area between the lower and the upper curves represents the contribution of NAPs. The area above the upper curve represents the contribution of CDOM.

experiment (Fig. 1). The contribution from the CDOM absorption coefficient to the total absorption coefficient is higher than 50%. Thus the CDOM is the main light-absorbing component at 443 nm. Note that similar results were obtained for the New England [22] and South Atlantic Bight shelf waters [23]. The phytoplankton and NAP contribution is around 24% and 22%, respectively, with rather stable values for phytoplankton.

Almost similar ratios were obtained for the Baltic Sea and, to a lesser extent, for the North Sea [8]. Previous studies regarding coastal waters showed that $a_{ph}(443)$ could be either greater than $a_{NAP}(443)$ [22,24,25] or lower [23]. Such a difference could be related to geographic peculiarities of the regions. For instance, the increase of NAP contribution to total particulate absorption is usually observed near the estuaries and is often related to the increase of terrigenous particles [23]. As well, episodic events

such as storms or hurricanes can lead to an increase of NAP contribution to the particulate absorption by a factor of 3–4 because of the resuspension [22,26]. The contribution of NAPs to the total particulate absorption at 443 nm could also be changed by a factor of 2–3 during a phytoplankton bloom and during postbloom periods [27]. Consequently, in the coastal waters, the variability in $a_{NAP}(443)$ and the contribution of $a_{NAP}(443)$ to the total particulate absorption show a regional specificity.

B. Phytoplankton Pigment Absorption as a Function of Chlorophyll A Concentration

1. Shape of the Relationship between a_{ph} and $Chla$

The analysis of a great number of measurements provided by [6] demonstrated that a nonlinear

relationship between the particulate absorption coefficient and the chlorophyll a concentration can be approximated using a power-law function. Further, Bricaud *et al.* [7] proposed a more relevant parameterization for the phytoplankton absorption coefficient when dealing with Case I water:

$$\alpha_{\text{ph}}(\lambda) = A_{\text{ph}}(\lambda) \text{Chl}^{E_{\text{ph}}(\lambda)}. \quad (2)$$

The coefficients $A_{\text{ph}}(\lambda)$ and $E_{\text{ph}}(\lambda)$ can be obtained through the linear fitting between logarithms of the absorption $\ln \alpha_{\text{ph}}(\lambda)$ and the concentration $\ln \text{Chl}$ of pigments for each wavelength λ :

$$\begin{aligned} A_{\text{ph}}(\lambda) &= \exp(\overline{\ln \alpha_{\text{ph}}(\lambda)} - E_{\text{ph}}(\lambda) \overline{\ln \text{Chl}}), \\ E_{\text{ph}}(\lambda) &= \frac{(\overline{\ln \alpha_{\text{ph}}(\lambda)} - \overline{\ln \alpha_{\text{ph}}(\lambda)})(\overline{\ln \text{Chl}} - \overline{\ln \text{Chl}})}{(\overline{\ln \text{Chl}} - \overline{\ln \text{Chl}})^2}, \end{aligned} \quad (3)$$

where the notation of parameters with an overbar means ensemble averaging.

The same approach as in the Bricaud *et al.* study [7] was applied to the Black Sea data. The spectral distribution of the absorption coefficient as a function of Tchl_a was then determined. The data set used in our study was obtained for a relatively short period of time, and the values of Tchl_a range from 0.45 up to 2.04 mg/m³. This is much less than in [7], where the chlorophyll concentration varied by a factor of 500. The scatterplot of the phytoplankton absorption coefficients at 440 nm (Fig. 2) shows that the nonlinear effect observed in the data of Bricaud *et al.* [7] is not pronounced here. However, we have used the power-law fitting, as it is additional “*a priori*” information obtained and validated earlier by Bricaud

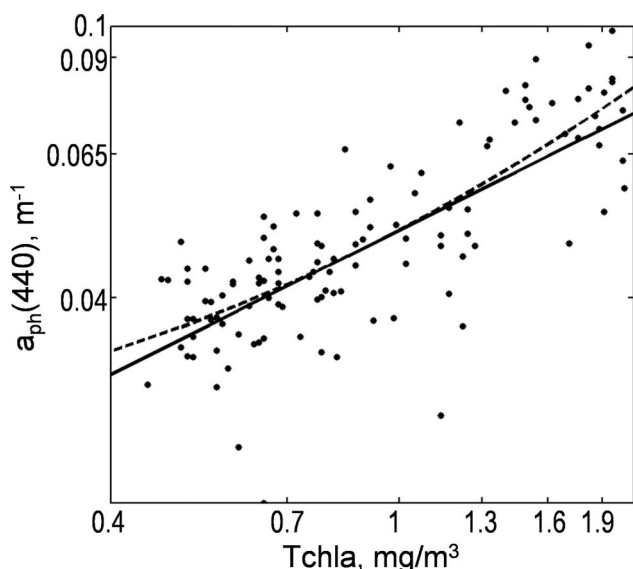


Fig. 2. Log–log scatterplot of the phytoplankton absorption coefficients at 440 nm versus Tchl_a. The linear regression line is presented as a dashed curve, and the log–log regression is plotted using the solid line.

et al. on the basis of the large number of measurements. Another reason is that it describes well the behavior of the absorption coefficient for the values of chlorophyll concentration outside the range of our measurements.

It is known that fitting nonlinear functions is less stable than fitting a linear function. This becomes more important in our case since the number of samples is limited (132 samples in total). Therefore special attention should be paid to the assessment of the stability and the statistical significance of the obtained estimates. Such an assessment is carried out in the following subsections.

2. Statistical Distribution of the Measurements and Estimation of Confidence Intervals

The results of fitting the Black Sea absorption data set together with the similar fitting presented in [7] are shown in Fig. 3. The numerical values of the fitting parameters are tabulated in Table 1 with a spectral resolution of 10 nm. The complete values can be obtained from the authors upon request. It is observed that the simple least-squares fit with a power-law function induces a spectral distribution of the estimated parameters, which is rather noisy [Figs. 3(a) and 3(b)]. It is necessary to identify the variations showing a statistical significance. The coefficients $A_{\text{ph}}(\lambda)$ and $E_{\text{ph}}(\lambda)$, which are derived from the statistical fitting, are considered as random values. To check whether the difference between our fitting and the parameterization proposed by Bricaud *et al.* [7] is not a result of stochastic fluctuations, the confidence intervals for the coefficients $A_{\text{ph}}(\lambda)$ and $E_{\text{ph}}(\lambda)$ need to be estimated. Because most of the frequently used efficient estimates and statistical tests are based on the assumptions of Gaussian distribution of the data, it was necessary to check first whether the statistical distribution of $\ln \alpha_{\text{ph}}(\lambda)$ and $\ln \text{Tchl}_a$ is consistent with a normal distribution. Two tests were used for that purpose. The first one is the Jarque–Bera test [28]. This test is based on the hypothesis that samples from the normal distribution have an expected skewness value of 0 and an expected kurtosis value of 3. The second test, the so-called Lilliefors test [29], uses as the statistics the maximum discrepancy between the empirical distribution function and the cumulative distribution function of the normal distribution with the estimated expectation and variance. So the Lilliefors test is just an adaptation of the Kolmogorov–Smirnov test [30] to the case where the parameters of normal distribution are not specified. Based on these tests, the hypothesis that the variables $\ln \text{Tchl}_a$ and $\ln \alpha_{\text{ph}}(\lambda)$ follow a normal distribution (Fig. 4) can be rejected with a probability of 0.95 for most of the wavelengths. Thus one cannot successfully apply the standard methods for constructing confidence intervals that are commonly based on student’s distribution or F distribution (see [31] for a complete description of the standard statistical methods).

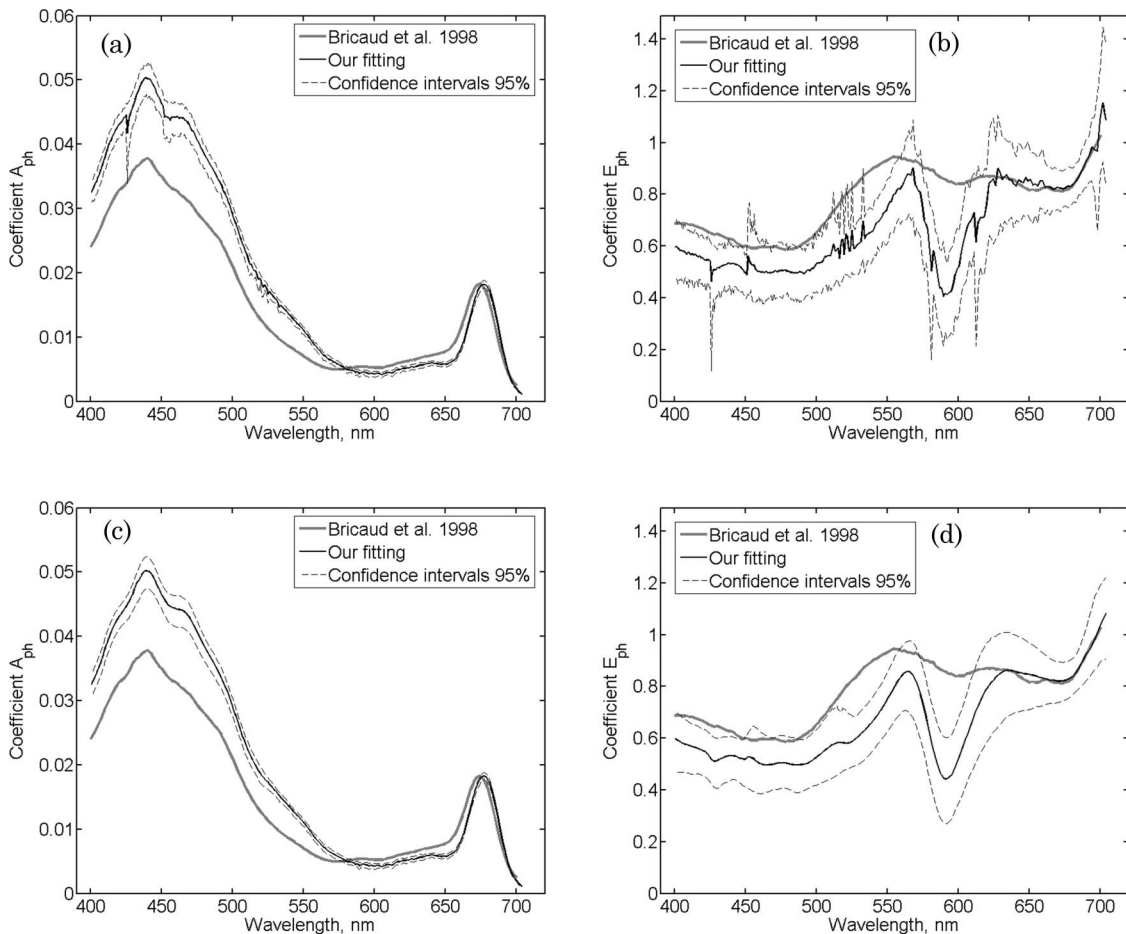


Fig. 3. Spectral values of the numerical coefficients (a) $A_{ph}(\lambda)$ and (b) $E_{ph}(\lambda)$ defining the parameterization of light absorption by phytoplankton as a function of Tchla. (c), (d) Similar to (a) and (b), except the modified local regression smoothing was used to remove the spurious high-frequency variability. Thick black lines are used for our fitting, thick gray lines represent the results obtained by Bricaud *et al.* [7], and dashed black lines represent 95% confidence intervals.

Therefore the so-called “bootstrap method” [32] was used to estimate the confidence intervals for coefficients $A_{ph}(\lambda)$ and $E_{ph}(\lambda)$.

Parametric techniques calculate a distribution function of the estimated parameter from the distribution function of the population, which is supposed to be known. In contrast, the bootstrap method allows us to estimate confidence intervals without this latter hypothesis. The bootstrap method is based on the generation of several ensembles of samples (so-called bootstrap samples) using the original measurements. Each bootstrap sample is created using a random sampling of the measured data. Every sample is returned to the original data set after selection. Therefore, when constructing a bootstrap sample, a particular data point from the original data set could appear multiple times. Using the various generated bootstrap samples, the procedure allows us to resample the coefficients $A_{ph}(\lambda)$ and $E_{ph}(\lambda)$ as many times as we need for the construction of an empirical cumulative distribution function that enables us to establish the uncertainty of those quantities. The confidence intervals constructed in such a way using 200 bootstrap samples are also shown in Figs. 3(a)

and 3(b). The results point out that the difference between the $A_{ph}(\lambda)$ and the $E_{ph}(\lambda)$ coefficients derived from the Black Sea measurements and those derived from [7] cannot be explained by a poor statistic, and thus the observed difference is statistically meaningful.

Figures 3(a) and 3(b) also show that all high spectral perturbations occurring within a resolution of 20 nm remain inside the confidence intervals, and thus these perturbations are statistically not significant. Therefore a low-pass filter was applied to remove the spurious harmonics. This filter is based on the local regression smoothing procedure proposed by Cleveland and Devlin [33]. This procedure employs the weighted second degree polynomial fitting in a moving interval. The weights are evaluated to adapt the moving interval to the irregular wavelength step and to make the solution robust to possible outliers. The Cleveland and Devlin [33] procedure was modified here to better account for the spectral variations of the parameters. The modification that was carried out in the current study consists of setting the spectral variability of the span (the key parameter of the local regression smoothing)

Table 1. Numerical Values of the Coefficients Used for the Parameterizations of Phytoplankton and Particulate Absorption Coefficients^a

Wavelength (nm)	$A_{ph}(\lambda)$	$E_{ph}(\lambda)$	$A_p(\lambda)$	$E_p(\lambda)$
400.47	0.033	0.597	0.119	0.378
411.00	0.039	0.570	0.118	0.393
421.39	0.043	0.547	0.115	0.401
431.58	0.048	0.518	0.112	0.411
442.27	0.050	0.531	0.107	0.421
452.68	0.045	0.527	0.097	0.394
462.73	0.044	0.497	0.092	0.382
473.24	0.041	0.504	0.085	0.385
483.31	0.037	0.498	0.077	0.379
493.81	0.033	0.503	0.069	0.380
504.78	0.026	0.548	0.059	0.393
515.18	0.020	0.583	0.050	0.406
526.02	0.017	0.591	0.043	0.427
536.17	0.014	0.644	0.038	0.450
546.72	0.012	0.721	0.032	0.480
557.70	0.009	0.824	0.027	0.499
567.83	0.007	0.844	0.022	0.505
578.34	0.005	0.650	0.019	0.474
589.25	0.004	0.446	0.017	0.434
600.57	0.004	0.530	0.015	0.434
610.84	0.004	0.684	0.013	0.458
621.47	0.005	0.803	0.013	0.502
632.48	0.006	0.860	0.013	0.540
643.88	0.006	0.852	0.012	0.561
653.98	0.006	0.841	0.011	0.588
664.41	0.010	0.825	0.015	0.660
675.18	0.018	0.823	0.022	0.725
686.30	0.012	0.886	0.016	0.754
697.79	0.003	1.006	0.005	0.649
703.69	0.001	1.081	0.003	0.518

^aThe data are provided with a spectral resolution of 10 nm. The complete values can be obtained from the authors upon request.

by employing the confidence intervals smoothed with a running mean. The proposed method preserves well the low-frequency variability of the extracted signal. The final spectral distribution of the coefficients $A_{ph}(\lambda)$ and $E_{ph}(\lambda)$ are shown in Figs. 3(c)

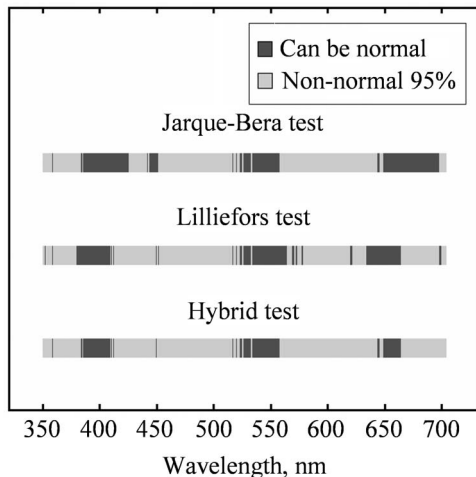


Fig. 4. Tests of normal distribution for $\ln \alpha_{ph}(\lambda)$. The upper bar represents the results of the Jarque–Bera test, the middle bar represents the Lilliefors test, and the lower bar corresponds to the hybrid test. The significance level is 0.05.

and 3(d) together with the confidence intervals. It is observed that the overall spectral shapes of the parameters calculated for the Black Sea waters and for the Case I waters are nearly similar, especially for A_{ph} . The correlation coefficients between our data and the Bricaud *et al.* study [7] are 0.99 and 0.76 for $A_{ph}(\lambda)$ and $E_{ph}(\lambda)$, respectively. Therefore, in the particular case where the values of Tchla are close to 1 mg m^{-3} , the calculation of phytoplankton absorption coefficient based on Eq. (2) is fairly independent of $E_{ph}(\lambda)$, and thus the spectral shape of absorption by phytoplankton in the Crimea coastal zone is almost identical to the shape found in deep-water regions by Bricaud *et al.* [7].

3. Comparison of Parameterizations

The values of $A_{ph}(\lambda)$ in the spectral range of 412–555 nm are greater than those derived using the parameterization of Bricaud *et al.* [7] [Fig. 3(c)]. Such behavior was already observed in other coastal regions like the Baltic Sea, the Adriatic Sea, and the English Channel [8]. In the present study, the relative concentration of phaeopigments is much lower than in the North Sea (the ratio Phaeo/Tchla is 23.7%) and may not explain the overestimation of the phytoplankton absorption coefficient in the blue when compared with Case I water parameterization. Here the peculiarities of the light absorption by the phytoplankton at short wavelengths in Crimea coastal waters are likely related to a higher ratio of accessory pigments related to chlorophyll a, as it was already observed in the Adriatic Sea [8]. The relatively higher ratio of accessory pigments is supposed to reflect the intracellular content of photoprotective pigments in summer.

In contrast with $A_{ph}(\lambda)$, the $E_{ph}(\lambda)$ values derived from our fitting are smaller than those derived from the Bricaud *et al.* [7] study in nearly the entire visible region [Fig. 3(d)]. All the exponents of the power-law function derived from our measurements are less than unity, which means a decrease of the chlorophyll-a-specific absorption coefficients with increasing Tchla. Such a type of function agrees with results obtained in open ocean waters [6,7,24,25,34,35] and more recently in the deep water region of the Black Sea [36]. In contrast with the results reported in [7], our fitting of $E_{ph}(\lambda)$ reveals a strong minimum around the 580 nm wavelength. Based on the confidence intervals, the minimum observed at 580 nm is statistically significant. The existence of this minimum means that the spectral shape of the phytoplankton absorption in the Crimea coastal zone is significantly different from the shape found in the open ocean waters. Within the range of Tchla measured during the Black Sea experiment, the influence of the coefficient $E_{ph}(\lambda)$ on the parameterization of $\alpha_{ph}(\lambda)$ is moderate. On the basis of Eq. (2), the major impact of the differences observed in $E_{ph}(\lambda)$ values between Case II and Case I waters would be observed at extremely high (typically when

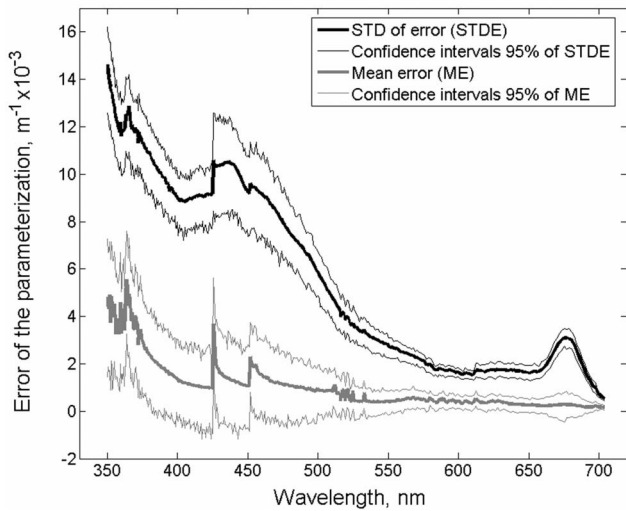


Fig. 5. Spectral distribution of the mean and random errors (the random error is defined as the standard deviation of the error) of the absorption parameterization of $a_{ph}(\lambda)$.

Tchla is more than 10 mg/m^3 or low (typically when Tchla is less than 0.1 mg/m^3) chlorophyll concentrations. In effect, the coefficient $E_{ph}(\lambda)$ varies from 0.4 to 0.8 within the spectral range around the minimum. The term $\text{Chl}^{E_{ph}(\lambda)}$, which is used in the parameterization [see Eq. (2)], varies by a factor of 2.5 when Tchla ranges from 0.1 to 10 mg/m^3 and only by a factor of 1.3 when Tchla varies within the interval from 0.45 to 2.04 mg/m^3 corresponding to our data set.

4. Analysis of Errors

Together with the confidence intervals, the error of the parameterization was estimated using the

leave-one-out cross validation method [31]. This method simulates the use of the parameterization with unknown data by (i) repeating the fitting procedure on the data subsets and then (ii) estimating the error on the data portions left out of each of these subsets. The mean value of this error can be interpreted as the systematic bias of the absorption parameterization, while the standard deviation characterizes the random error. The spectral variations of these errors (i.e., mean and random errors) are presented in Fig. 5. At all wavelengths, the random error is significantly higher than the mean error. In the green–red spectral region, the variations of random error are in agreement with the spectral variations of the absorption coefficient. With decreasing wavelength, the situation changes, and both errors increase. High values of the relative error of the absorption coefficient are observed in the UV spectral region, which is especially important at low values of chlorophyll concentrations. At the same time, the broadening of confidence intervals suggests a possible instability in the shortwave area. So it is likely that the constructed parameterization is questionable at wavelengths shorter than 400 nm.

The high values of the root mean square error (RMSE) of the parameterization of $a_{ph}(\lambda)$ suggest that perhaps pigment concentrations may not be the single parameter influencing the light absorption by phytoplankton. Figure 6(a) shows how $a_{ph}(\lambda)$ changes when Tchla has a fixed value, namely, 0.65 mg/m^3 . Variations of $a_{ph}(\lambda)$ are greater than the RMSE interval estimated for the entire range of concentrations available in our data set. The magnitude of these variations is comparable with the magnitude of variations that would be due to changes in chlorophyll concentration. Since the

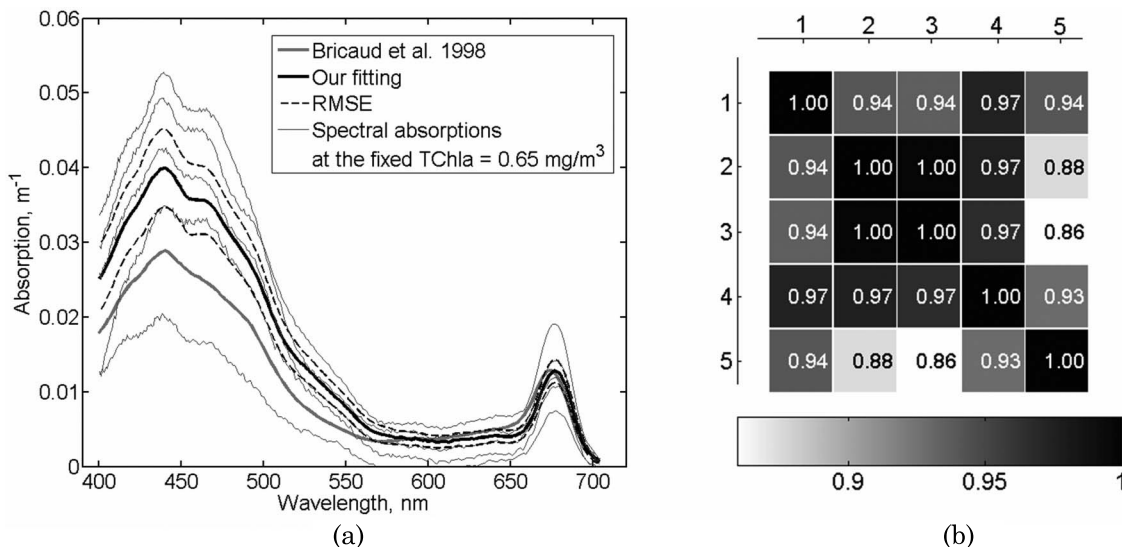


Fig. 6. Variations of the spectral absorption coefficient of phytoplankton for a fixed value of Tchla, namely, 0.65 mg m^{-3} . In (a), the thick gray curve represents the parameterization of phytoplankton absorption coefficient proposed by Bricaud *et al.* [7], and the thick black curve is the parameterization obtained based on our data set. The thin gray curves (five in total) are spectral absorption coefficients measured for different waters at the fixed chlorophyll concentration value of 0.65 mg/m^3 . The correlation coefficients between these five curves are represented in (b).

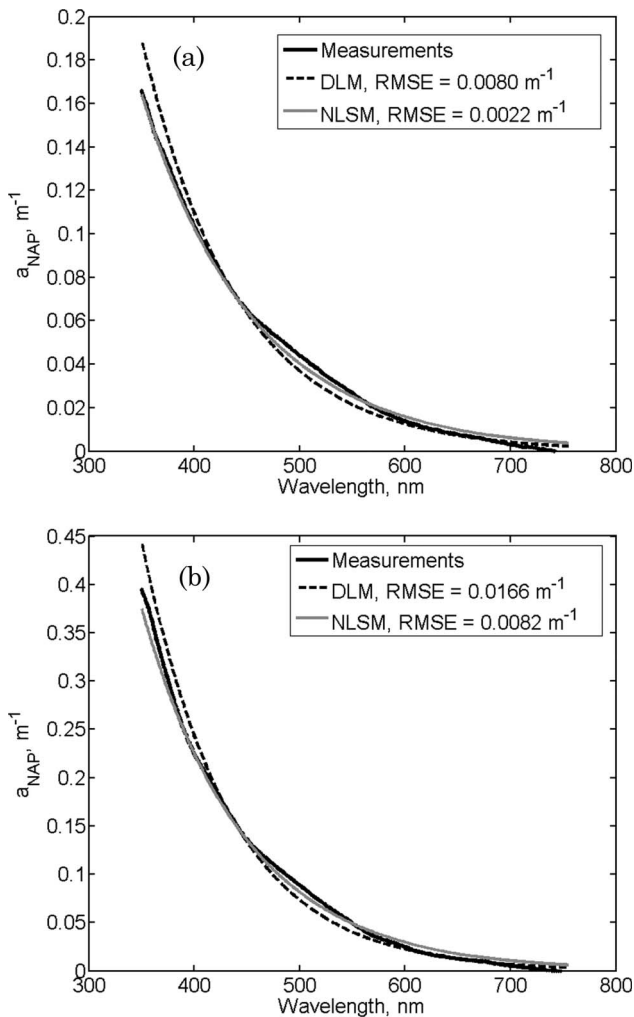


Fig. 7. Examples of the exponential fit of the NAP spectral absorption coefficient using different methods for (a) a case representing the fit for which the error is close to its typical value (sample collected on 28 July 2002, depth 8 m) and (b) a case corresponding to the greatest error made by the NLSM fitting (sample collected on 14 August 2002, depth 16 m).

variations of $a_{ph}(\lambda)$ are significant at all wavelengths, those variations are not attributed to potentially incorrect measurements in the UV range. The strong variations of a_{ph} given a *Tchl*a concentration are probably related to the variability in phytoplankton species throughout the “packaging effect,” which consists of variations of pigment absorption properties due to the nonuniform distribution of pigments within the phytoplankton cells [37]. Morel and Bricaud [37] demonstrated that the packaging effect is a major source of variability in the absorption coefficients of phytoplankton species. Figure 6(b) demonstrates that the correlation coefficients between the five plots of spectral values of $a_{ph}(\lambda)$ measured at the same *Tchl*a are high and show a minimum value of 0.86. This means that the absorption spectra do not have significant differences in shape. In other words, one absorption spectrum can be derived from another one using a linear correction. Such a result

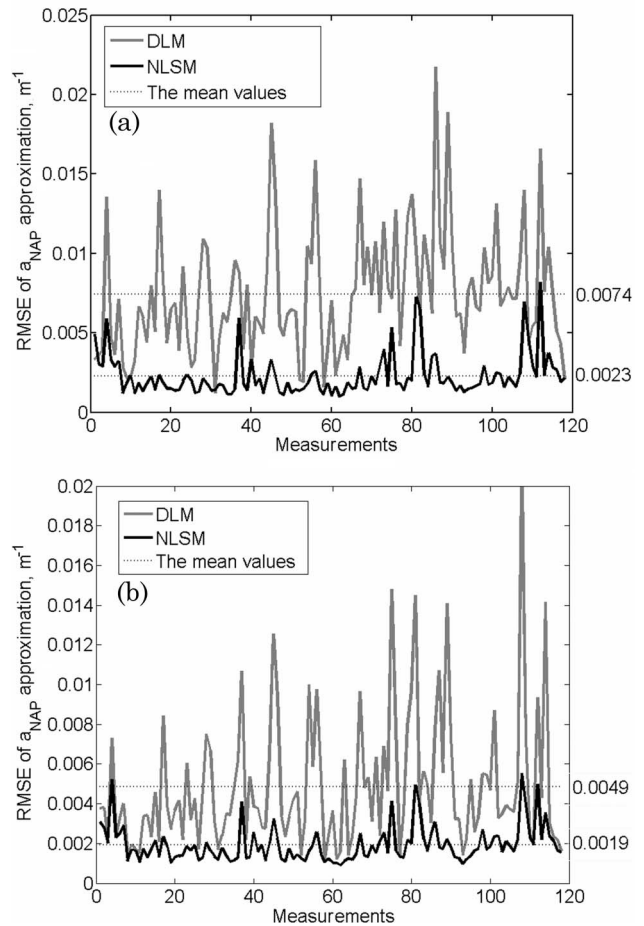


Fig. 8. RMSE of DLM (solid gray curve) and NLSM (solid black curve) for all the measurements (a) when the fitting is carried out in the spectral region from 380 to 730 nm, excluding the intervals 400–480 and 620–710 nm, and (b) when the fitting is performed using the entire spectral region from 350 to 700 nm.

suggests that a more precise parameterization of phytoplankton absorption spectra specific for coastal areas might be obtained. However, more investigation is required at this point, and this aspect will not be analyzed here.

C. Absorption Properties of Nonalgal Particles, Total Particulate, and Colored Dissolved Organic Matter

1. Influence of the Fitting Method on $a_{NAP}(\lambda)$ Parameterization

It is commonly believed that the NAP absorption spectra can be parameterized using an exponential fit for different coastal waters [8]. The expression for the spectral absorption coefficient is written as follows:

$$a_{NAP}(\lambda) = \tilde{a}_{NAP}(\lambda_r) e^{-S_{NAP}(\lambda - \lambda_r)}, \quad (4)$$

where $\tilde{a}_{NAP}(\lambda_r)$ is a known (measured or simulated) value of absorption coefficient at the reference wavelength λ_r . The unknown exponential slope parameter

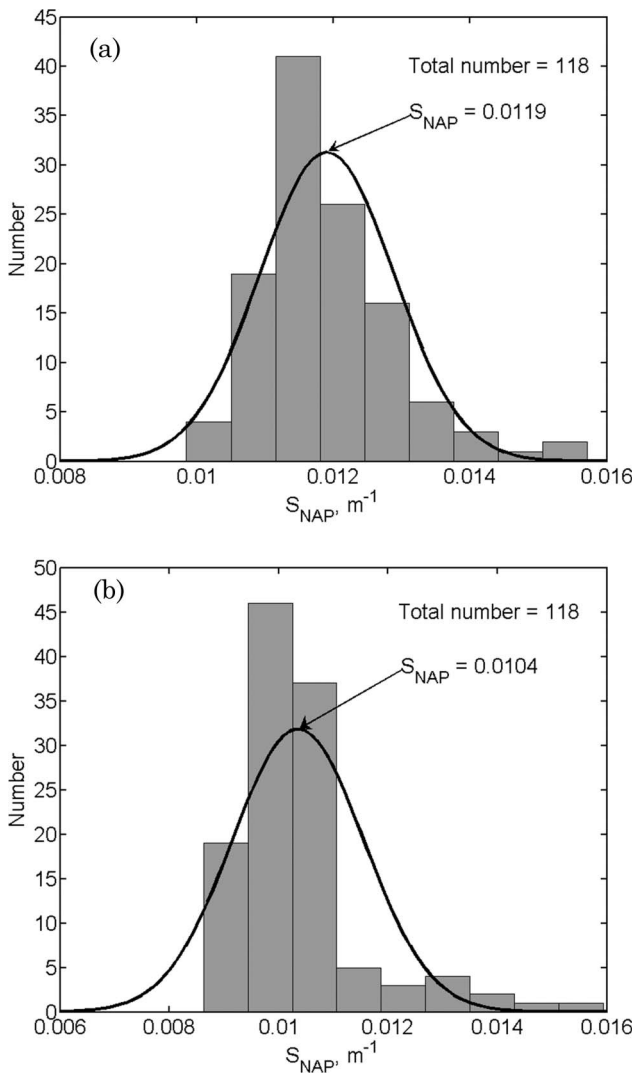


Fig. 9. Histograms of the exponential slope parameter S_{NAP} for the parameterization of the NAP absorption coefficient. The fitting is performed in the spectral region from 380 to 730 nm, excluding the intervals 400–480 and 620–710 nm using two different methods: (a) DLM and (b) NLSM. Black curves show the probability density functions of the normal distribution fitted to the corresponding data and scaled to the histograms.

S_{NAP} can be found using some optimization method. The same approximation is applied here for the parameterization of $a_{\text{NAP}}(\lambda)$ in the Black Sea coastal waters. In general, the exponential law fits well the observed spectra, but the previous investigations [8] showed that the error due to such parameterization varies significantly for different waters. One of the possible reasons given by Babin *et al.* [8] is the influence of any residual pigment absorption. Thus Babin *et al.* [8] suggested an exponential fit for the spectral region ranging from 380 to 730 nm, excluding the intervals of 400–480 and 620–710 nm.

In this paper, two different techniques of exponential fitting were applied: one is based on the data linearization method (DLM) [38], and the other is based on the numerical minimization of the functional error (the nonlinear least-square method [NLSM]) [38].

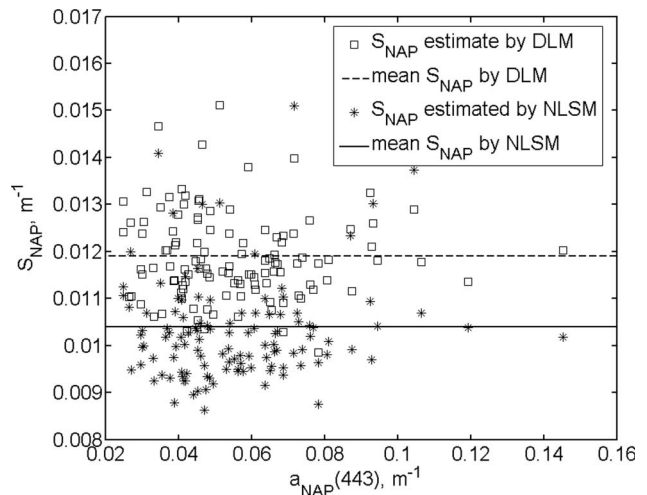


Fig. 10. Scatterplots of the slope parameter S_{NAP} estimated by the DLM (squares) and by the NLSM (stars), with respect to the NAP absorption coefficient at the reference wavelength 443 nm. Black solid and dashed lines show the corresponding mean values of S_{NAP} .

The mean values of the RMSE are quite different for these methods, namely, 0.0074 and 0.0023 m^{-1} for DLM and NLSM, respectively. An example showing one of the cases where RMSE has a typical value is presented in Fig. 7(a). Both methods systematically induce an underestimate of the absorption measurements in the spectral range of 450–550 nm and an overestimate of the data in the range of 680–750 nm. However, in the UV spectral region, the behavior of DLM and NLSM approximations does not show any systematic underestimate or overestimate of the data. This is probably because the measurements showed the highest variability in the UV part of the spectrum. The comparison of the performance of DLM and NLSM is now carried out based on a representative case for which the fitting error of the absorption spectra retrieval is the highest [Fig. 7(b)]. For such a case, the mean values of the relative RMSE are 12% and 7% for DLM and NLSM, respectively. Therefore the NLSM appears to be a more accurate technique than the DLM. This can be explained by the fact that the sensitivity of the fitting carried out using the NLSM to the spectral variations of the optical parameters does not depend on the wavelength, while the DLM takes into account the spectral dependency of these parameters due to the linearization approach. As a result, the NLSM is more robust and appropriate for parameterizing absorption coefficients of marine particles.

The values of the RMSE obtained for all the samples are shown in Fig. 8(a). As expected from the analysis of the sample shown in Fig. 7(b), it is observed that the RMSE values derived using the parameterization of $a_{\text{NAP}}(\lambda)$ obtained with the NLSM are significantly lower than those derived when using the DLM. Furthermore, the variability in the DLM error is high, with a value of 0.0039 m^{-1} , which is much greater than the value of the standard deviation

obtained for the NLSM error, namely, 0.0013 m^{-1} . Figure 8(b) shows the values of the RMSE when the calibration of the methods is performed at wavelengths ranging from 350 to 700 nm without excluding any spectral intervals. The mean RMSE value is 0.0019 m^{-1} for NLSM, which is nearly similar to the value obtained for the case when spectral intervals were excluded (i.e., 0.0023 m^{-1} , Fig. 8(a)). On the other hand, the mean RMSE value obtained for the DLM considerably decreased down to 0.0049 m^{-1} (i.e., decreased by a factor of 1.5) when the entire spectral range is considered relative to the case where spectral intervals are excluded. This is because the additional spectral information provided by the full visible spectrum reduces the number of ambiguities for the fitting and thus leads to more accurate fitting parameters. Based on the results shown in Fig. 8, it can be concluded that the performances of the NLSM are still satisfactory when considering all wavelengths for fitting the measurements. Such an approach is then weakly sensitive to the influence of any residual pigment absorption as the standard exponential law fits could be [8]. Therefore the NLSM is an efficient method recommended to correctly parameterize the NAP absorption coefficient.

2. Estimation of the Exponential Slope Parameter

The significance of the difference between the slope parameters of the exponential fit (S_{NAP}) obtained by the fitting methods considered in this paper was also studied. We constructed the histograms of S_{NAP} and fitted the probability density functions of the normal distribution for each of these two methods [Figs. 9(a) and 9(b)]. The slope parameter of the exponential fit S_{NAP} varies from 0.0099 to 0.0157 nm^{-1} for the DLM and from 0.0086 to 0.0159 nm^{-1} for the NLSM, which is in agreement with the results obtained by Babin *et al.* [8]. We were not able to find any significant correlation between the slope parameter and the absorption coefficient at the reference wavelength 443 nm, as well as some apparent nonlinear relationship (Fig. 10). Thus the uncertainty in S_{NAP} cannot be reduced using $a_{\text{NAP}}(443)$. Therefore the mean S_{NAP} value was used in the parameterization of NAP absorption. In the latter case, the uncertainty in the parameterization can be defined as two or three times the value of the standard deviation of S_{NAP} , which is equal to 0.001 m^{-1} for the DLM and 0.0012 m^{-1} for the NLSM. The difference of mean values of S_{NAP} obtained by the DLM and the NLSM is significant and exceeds the value of the standard deviation. Note also that the difference between mean values of S_{NAP} for the DLM and the NLSM is greater than the range of the average slopes obtained for different waters represented in [8]. The problem of the choice of the exponential fitting method is really important for constructing the parameterization of the NAP absorption coefficient, and thus it is necessary to decide

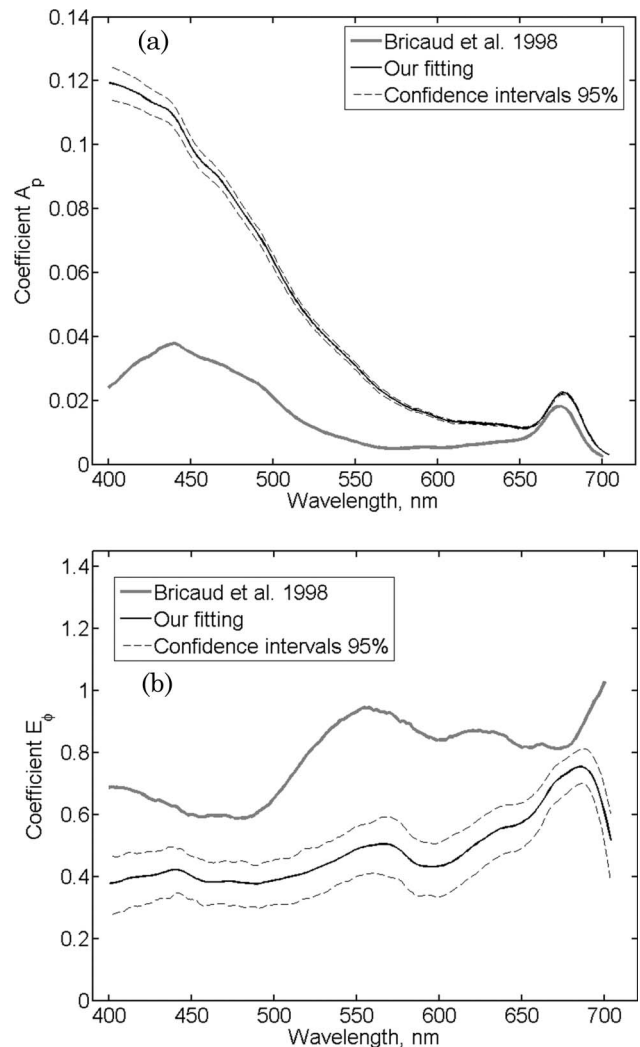


Fig. 11. Spectral values of the numerical coefficients (a) $A_p(\lambda)$ and (b) $E_p(\lambda)$ used in the parameterization of the total particulate absorption coefficient as a function of Tchl_a. Thick black lines represent the results of the current study, thick gray lines represent results obtained in the Bricaud *et al.* study [7], and thin gray lines represent the confidence intervals at 95%.

which of the tested methods is most suitable. Based on the results discussed in Subsection 3.C.1 (see Fig. 8), the use of the NLSM is clearly more appropriate. The NAP absorption coefficient could be parameterized as

$$a_{\text{NAP}}(\lambda) = a_{\text{NAP}}(443)e^{(-0.0104 \pm 0.0024)(\lambda - 443)}. \quad (5)$$

3. Parameterization of the Total Particulate Spectral Absorption Coefficient

The relationship between the particulate absorption coefficient a_p and the total phytoplankton pigment concentration for the Crimea coastal zone was also investigated using the method proposed in [7] (see Subsection 3.B.1). The spectral distribution of coefficients $A_p(\lambda)$ and $E_p(\lambda)$ was calculated using the

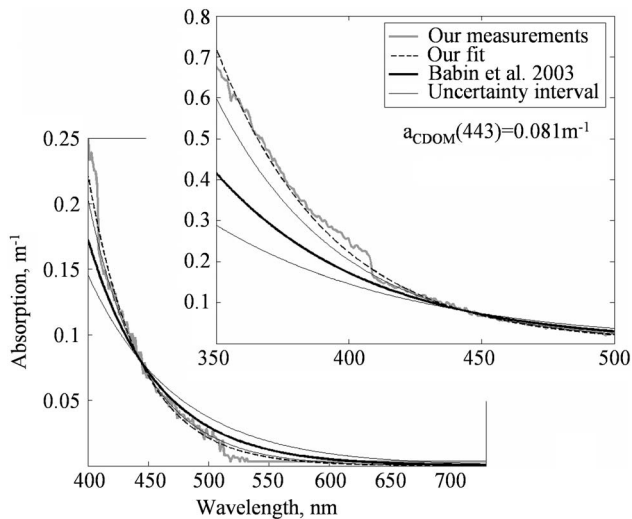


Fig. 12. Exponential fitting of the CDOM absorption coefficient using the NLSM. The gray curves represent the measurements of the CDOM absorption coefficient obtained on 3 August 2002 (surface), the dashed curves show the proposed fitting calculated over the spectral region from 350–500 nm, the thick and thin black solid curves show the a_{CDOM} parameterization proposed by Babin *et al.* [8] with uncertainty intervals.

log–log regression technique [Figs. 11(a) and 11(b)]. The numerical values of these coefficients are tabulated Table 1. The confidence intervals (95%) were constructed using the bootstrap method.

The comparison with the fitting of Bricaud *et al.* [7] clearly shows that the spectral distributions of coefficients $A_p(\lambda)$ and $E_p(\lambda)$ are not so similar in magnitude (much greater values in our case) and in shape, as it was highlighted for the parameterization of absorption by phytoplankton. The highest difference can be observed in the UV green spectral region, while the parameterizations in the red spectral region are fairly consistent. Obviously the discrepancy between our parameterization and that of Bricaud *et al.* [7] cannot be explained by instability owing to the small number of samples. The discrepancy is probably due to the high content of NAPs, which is much more important here (around 50%) than in Case I waters. Such a high content of NAPs is expected in coastal areas, owing to rivers inputs. The decrease of the discrepancy with parameterization of Bricaud *et al.* [7] around 678 nm can be explained by a minor contribution of NAPs to a_p in this spectral region.

4. Variability in the Colored Dissolved Organic Matter Absorption Coefficient

The water samples dedicated to the CDOM measurements were collected at the sea surface within the entire period of data acquisition on 2, 3, 10, and 14 August 2002. The magnitude of the CDOM absorption coefficient at 443 nm $a_{\text{CDOM}}(443)$ ranges from 0.081 m^{-1} (on 3 August 2002) to 0.197 m^{-1} (on 14 August 2002) and changes by more than a factor of 2 during the field experiment, with a significant

increase after the wind-gusting event that occurred a few days after the beginning of the sampling [14]. The mean value of $a_{\text{CDOM}}(443)$ (0.13 m^{-1}) is close to values measured in the North Sea and remains within the interval of the whole variability of this parameter, namely, 0.01–0.6 m^{-1} found in various coastal waters around Europe [8]. The $a_{\text{CDOM}}(443)$ values obtained in the Black Sea are consistent with the cross-shelf measurements in the South Atlantic Bight (0.02–0.4 m^{-1}) [23] but remain lower than the data obtained in the New England shelf waters (0.060–0.081 m^{-1}) [22].

The CDOM absorption spectra $a_{\text{CDOM}}(\lambda)$ were fitted in the spectral range of 350–500 nm [8] using an exponential function:

$$a_{\text{CDOM}}(\lambda) = \tilde{a}_{\text{CDOM}}(\lambda_r) e^{-S_{\text{CDOM}}(\lambda - \lambda_r)}, \quad (6)$$

where $\tilde{a}_{\text{CDOM}}(\lambda_r)$ is a known value of the absorption coefficient at the reference wavelength λ_r . In this case, the exponential slope parameter can also be estimated by both the DLM and the NLSM. It should be noted that fitting by the DLM was used for CDOM absorption spectra modeling mainly in earlier papers, for instance, in [39]. The comparison of the DLM and the NLSM for the parameterization of absorption by chromophoric dissolved organic matter for Danish coastal waters was provided by Stedmon *et al.* [40]. It was shown that, in spite of the fact that both estimates using linearized and nonlinear fittings exhibit a high correlation, the nonlinear method allows a much stronger reduction of the mean sum of absolute residuals, and it provides a more precise parameterization of $a_{\text{CDOM}}(\lambda)$. Further, this result was confirmed by Twardowski *et al.* [41], and now the NLSM is used for modeling $a_{\text{CDOM}}(\lambda)$ by most authors [42–44]. Since we do not have enough measurements in the considered region to provide an independent comparison of these methods, we chose the NLSM to estimate the spectral slope parameter S_{CDOM} , relying on the previous results. The derived mean value is 0.0179 nm^{-1} , which is in agreement with the overall estimates obtained by Babin *et al.* [8]. However, half of the spectral CDOM absorption measurements are not included within the uncertainty intervals constructed by Babin *et al.* [8] for the parameterization of CDOM absorption. As an example, Fig. 12 shows the measurements of $a_{\text{CDOM}}(\lambda)$ performed on 3 August 2002. Nevertheless, the absorption spectra could be correctly fitted using an exponential function. Thus the average slope parameter estimated from our measurements allows us to suggest the following expression for the absorption spectrum for the Crimea coastal zone:

$$a_{\text{CDOM}}(\lambda) = a_{\text{CDOM}}(443) e^{-0.0179(\lambda - 443)}. \quad (7)$$

However, since the number of data that were used to derive the parameterization of a_{CDOM} is very limited, it should be highlighted that our conclusion remains preliminary. Additional measurements are required

to calculate the uncertainty intervals of the proposed parameterization.

4. Conclusions

We have studied the absorption properties of phytoplankton and nonalgal and CDOMs for coastal seawaters. Our analysis is based on a data set of bio-optical measurements obtained during a field experiment carried out in the Crimea Peninsula (Black Sea, Ukraine). The absorption budget showed that Crimea coastal waters clearly fall into the Case II water type, with a yellow-substance-dominated regime. It was demonstrated that the use of current parameterization methods to estimate the spectral absorption coefficients of marine particles is not relevant under these circumstances. Therefore relevant parameterizations for modeling the particulate and phytoplankton absorption properties were proposed. The parameterizations of the particulate and phytoplankton absorption coefficients obtained using the simple power-law fitting suffered from the spurious noise. We proposed a combination of the simple power-law fitting with the modified local regression method based on a low-pass filter and bootstrapping. The bootstrap method allowed us to estimate confidence intervals for the parameterization coefficients in the case of non-Gaussian distributed samples of the particulate and phytoplankton absorption coefficients. The derived confidence intervals were then used to adjust the local regression filter for efficiently removing the spurious noise with the minimum underestimation of low-frequency variability. The parameterizations are relevant to coastal waters near the Crimea Peninsula and for chlorophyll *a* concentrations ranging from 0.45 up to 2.04 mg/m³.

The measurements of NAP and CDOM absorption coefficients were fitted using an exponential function. Two different techniques were tested and compared for estimating the slope parameter: the DLM and the NLSM. The sensitivity of the DLM to the choice of spectral intervals used for its calibration was significant. Thus the use of the DLM led to the instability of the parameterizations and to greater errors. In particular, it was shown that the NLSM is weakly sensitive to the influence of any residual pigment absorption, and thus the NLSM is more appropriate than the standard exponential law fits currently employed in coastal areas [8] to parameterize NAP absorption coefficients. Thus, to obtain S_{NAP} and S_{CDOM} , we chose the NLSM as the fitting method that appeared to be much more accurate and stable to estimate the slope parameters. Our estimate of the mean value of S_{NAP} is $0.0104 \pm 0.0024 \text{ nm}^{-1}$, which is significantly lower than the slopes derived by Babin *et al.* [8]. On the other hand, the mean value of $S_{\text{CDOM}} = 0.0179 \text{ nm}^{-1}$ is in good agreement with [8].

The results presented in this study clearly show that the Crimea coastal waters have their own optical particularities. We demonstrated that parameterizations established by other investigators do not fit

our data set, and this is not explained by variations due to a small number of measurements. The proposed methods allowed us to increase the accuracy and stability of the parameterizations of the spectral absorption coefficients for Case II water. The results discussed in this paper have important implications for ocean color research. The proposed methods and parameterizations will contribute to significantly improve the modeling of the inherent optical properties and thus the analysis of water-leaving radiances in optically complex waters, which are of great interest for satellite remote sensing applications.

This work was funded by the Centre National d'Etudes Spatiales (CNES), France, and by the Russian Foundation for Basic Research (projects 07-05-00328-a and 06-05-64916-a). The authors thank A. Kuznetsov, the director of the platform in Katsiveli, Ukraine. We are grateful to all the participants of the experiment: M. E.-G. Lee, G. A. Berseneva, E. B. Martynov, and M. Shybanov. The authors also thank A. Bricaud for helpful discussions. We dedicate this paper to the memory of G. Khomenko.

References

1. B. G. Mitchell and D. A. Kiefer, "Chlorophyll *a* specific absorption and fluorescence excitation spectra for light limited phytoplankton," *Deep-Sea Res.* **35**, 639–663 (1988).
2. M. Babin, J. C. Therriault, L. Legendre, and A. Condal, "Variations in the specific absorption coefficient for natural phytoplankton assemblages: impact on estimates of primary production," *Limnol. Oceanogr.* **38**, 154–177 (1993).
3. M. Babin, A. Morel, P. G. Falkowski, H. Claustre, A. Bricaud, and Z. Kobler, "Nitrogen- and irradiance-dependent variations of the maximum quantum yield of carbon fixation in eutrophic, mesotrophic and oligotrophic systems," *Deep-Sea Res.* **43**, 1241–1272 (1996).
4. D. Stramski, A. Bricaud, and A. Morel, "Modeling the inherent optical properties of the ocean based on the detailed composition of planktonic community," *Appl. Opt.* **40**, 2929–2945 (2001).
5. A. Morel and L. Prieur, "Analysis of variations in ocean color," *Limnol. Oceanogr.* **22**, 709–722 (1977).
6. A. Bricaud, M. Babin, A. Morel, and H. Claustre, "Variability in the chlorophyll-specific absorption coefficients of natural phytoplankton: analysis and parameterization," *J. Geophys. Res.* **100**, 13321–13332 (1995).
7. A. Bricaud, A. Morel, M. Babin, K. Allali, and H. Claustre, "Variations of light absorption by suspended particles with chlorophyll *a* concentration in oceanic (case 1) waters: analysis and implications for bio-optical models," *J. Geophys. Res.* **103**, 31033–31044 (1998).
8. M. Babin, D. Stramski, G. M. Ferrari, H. Claustre, A. Bricaud, G. Obolensky, and N. Hoepffner, "Variations in the light absorption coefficients of phytoplankton, nonalgal particles, and dissolved organic matter in coastal waters around Europe," *J. Geophys. Res.* **108**, 3211 (2003), doi:10.1029/2001JC000882.
9. M. Chami, E. B. Shybanov, T. Y. Churilova, G. A. Khomenko, M. E.-G. Lee, O. V. Martynov, G. A. Berseneva, and G. K. Korotaev, "Optical properties of the particles in the Crimea coastal waters (Black Sea)," *J. Geophys. Res.* **110**, C11020 (2005), doi:10.1029/2005JC003008.

10. M. Chami, E. Marken, J. J. Starnes, G. Khomenko, and G. Korotaev, "Variability of the relationship between the particulate backscattering coefficient and the volume scattering function measured at fixed angles," *J. Geophys. Res.* **111**, C05013 (2006), doi:10.1029/2005JC003230.
11. M. Chami, D. McKee, E. Leymarie, and G. Khomenko, "Influence of the angular shape of the volume scattering function and multiple scattering on remote sensing reflectance," *Appl. Opt.* **45**, 9210–9220 (2006).
12. M. Chami, E. B. Shybanov, G. Khomenko, M. Lee, O. V. Martynov, and G. Korotaev, "Spectral variation of the volume scattering function measured over the full range of scattering angles in a coastal environment," *Appl. Opt.* **45**, 3605–3619 (2006).
13. G. K. Korotaev, G. A. Khomenko, M. Chami, G. A. Bersevana, O. V. Martynov, M. E.-B. Lee, E. B. Shybanov, T. V. Churilova, A. S. Kuznetsov, and A. K. Kuklin, "International subsatellite experiment on the oceanographic platform," *Phys. Oceanogr.* **14**, 150–160 (2004).
14. T. Y. Churilova and G. P. Berseneva, "Absorption of light by phytoplankton, detritus, and dissolved organic substances in the coastal region of the black sea (July–August 2002)," *Phys. Oceanogr.* **14**, 221–233 (2004), in Russian.
15. G. S. Fargion and J. L. Mueller, "Ocean optics protocols for satellite ocean color sensor validation," NASA Tech. Memo. 2000-209966 (Goddard Space Flight Center, Greenbelt, MD, 2000).
16. O. Holm-Hansen, C. J. Lorenzen, R. W. Holmes, and J. D. H. Strickland, "Fluorometric determination of chlorophyll," *J. Cons. Cons. Int. Explor. Mer* **30**, 3–15 (1965).
17. C. F. Gibbs, "Chlorophyll b interference in the fluorometric determination of chlorophyll a and phaeopigments," *Aust. J. Mar. Freshwater Res.* **30**, 597–606 (1979).
18. G. Berseneva and T. Churilova, "Chlorophyll concentration and phytoplankton optical characteristics in shelf waters of the Black Sea near the Crimea," *Marine Hydrophys. J.* **2**, 44–57 (2001), in Russian.
19. T. Y. Churilova, G. P. Berseneva, and L. V. Georgieva, "Variability in bio-optical characteristics of phytoplankton in the Black Sea," *Oceanology* **44**, 192–204 (2004).
20. C. S. Yentsch, "Measurement of visible light absorption by particulate matter in the ocean," *Limnol. Oceanogr.* (Engl. Transl.) **7**, 207–217 (1962).
21. M. Kishino, N. Takahashi, N. Okami, and S. Ichimura, "Estimation of the spectral absorption coefficients of phytoplankton in the sea," *Bull. Mar. Sci.* **37**, 634–642 (1985).
22. H. M. Sosik and R. E. Green, "Temporal and vertical variability in optical properties of New England shelf waters during late summer and spring," *J. Geophys. Res.* **106**, 9455–9472 (2001).
23. J. R. Nelson and S. Guarda, "Particulate and dissolved spectral absorption on the continental shelf of the southeastern United States," *J. Geophys. Res.* **100**, 8715–8732 (1995).
24. J. S. Cleveland, "Regional models for phytoplankton absorption as a function of chlorophyll a concentration," *J. Geophys. Res.* **100**, 13333–13344 (1995).
25. H. M. Sosik and B. G. Mitchell, "Light absorption by phytoplankton, photosynthetic pigments, and detritus in the California current system," *Deep-Sea Res.* **42**, 1717–1748 (1995).
26. G. Berseneva and T. Churilova, "Chlorophyll concentration and phytoplankton optical characteristics in shelf waters of the Black Sea near the Crimea," *Marine Hydrophys. J.* **2**, 44–58 (2001), in Russian.
27. T. Churilova, G. Berseneva, L. Georgieva, and Y. Bryanzeva, "Bio-optical characteristics of phytoplankton in winter-spring "bloom" of the Black Sea," *Marine Hydrophys. J.* **5**, 28–40 (2001), in Russian.
28. A. K. Bera and C. M. Jarque, "Efficient tests for normality, homoscedasticity and serial independence of regression residuals," *Econ. Lett.* **6**, 255–259 (1980).
29. H. Lilliefors, "On the Kolmogorov–Smirnov test for normality with mean and variance unknown," *J. Am. Stat. Assoc.* **62**, 399–402 (1967).
30. A. N. Kolmogorov, "Confidence limits for an unknown distribution function," *Ann. Math. Stat.* **12**(4), 461–463 (1941).
31. D. S. Wilks, *Statistical Methods in the Atmospheric Sciences*, 2nd ed. (Elsevier Academic, 2006).
32. A. C. Davison and V. D. Hinkley, *Bootstrap Methods and Their Application* (Cambridge U. Press, 1997).
33. W. S. Cleveland and S. J. Devlin, "Locally-weighted regression: an approach to regression analysis by local fitting," *J. Am. Stat. Assoc.* **83**, 596–610 (1988).
34. S. Sathyendranath, T. Platt, V. Stuart, B. Irwin, M. J. W. Veldhuis, G. W. Kraay, and W. G. Harrison, "Some bio-optical characteristics of phytoplankton in the NW Indian Ocean," *Mar. Ecol. Prog. Ser.* **132**, 299–311 (1996).
35. S. Sathyendranath, V. Stuart, B. Irwin, H. Maass, G. Savidge, L. Gilpin, and T. Platt, "Seasonal variations in bio-optical properties of phytoplankton in the Arabian Sea," *Deep-Sea Res. II* **46**, 633–653 (1999).
36. T. Churilova, G. Berseneva, and L. Georgieva, "Variability in bio-optical characteristics of phytoplankton in the Black Sea," *Oceanology* **44**, 192–204 (2004).
37. A. Morel and A. Bricaud, "Theoretical results concerning light absorption in a discrete medium, and application to specific absorption of phytoplankton," *Deep-Sea Res.* **28**, 1375–1393 (1981).
38. J. H. Mathews and K. K. Fink, *Numerical Methods Using MATLAB* (Prentice Hall, 2004).
39. A. Bricaud, A. Morel, and L. Prieur, "Absorption by dissolved organic matter of the sea (yellow substance) in the UV and visible domains," *Limnol. Oceanogr.* **26**, 43–53 (1981).
40. C. A. Stedmon, S. Markager, and H. Kaas, "Optical properties and signatures of chromophoric dissolved organic matter (CDOM) in Danish coastal waters," *Estuar. Coast. Shelf Sci.* **51**, 267–278 (2000).
41. M. S. Twardowski, E. Boss, J. M. Sullivan, and P. L. Donaghay, "Modeling the spectral shape of absorption by chromophoric dissolved organic matter," *Mar. Chem.* **89**, 69–88 (2004).
42. Y. Zhang, B. Qin, G. Zhu, L. Zhang, and L. Yang, "Chromophoric dissolved organic matter (CDOM) absorption characteristics in relation to fluorescence in Lake Taihu, China, a large shallow subtropical lake," *Hydrobiologia* **581**, 43–52 (2007).
43. J. R. Helms, A. Stubbins, J. D. Ritchie, E. C. Minor, D. J. Kieber, and K. Mopper, "Absorption spectral slopes and slope ratios as indicators of molecular weight, source, and photobleaching of chromophoric dissolved organic matter," *Limnol. Oceanogr.* **53**, 955–969 (2008).
44. L. Retamal, W. F. Vincent, C. Martineau, and C. L. Osburn, "Comparison of the optical properties of dissolved organic matter in two river-influenced coastal regions of the Canadian Arctic," *Estuar. Coast. Shelf Sci.* **72**, 261–272 (2007).